

(which account for one-half of the antioxidant capacity of plasma) (15), of vitamin E (carried in lipoproteins together with cholesterol) and other antioxidants (16), and in sepsis, with reduced antioxidant protection by sulfur amino acids (17). In sepsis, it is also related to impaired energy and amino acid disposal, which is partly reversed by increasing the amino acid supply (2, 18). Recent studies also suggest that cholesterol becomes an essential substance in extreme illness (19). At present, however, the main clinical implication of severe hypocholesterolemia in acute states is the need for rapid treatment and resolution of the underlying illness.

We acknowledge the kind assistance of Maurizio Cianfanelli (Catholic University Medical School) and Rosaria Di Pasquale, nurse and sister of a nonsurviving patient.

## References

- Alvarez C, Ramos A. Lipids, lipoproteins, and apoproteins in serum during infection. *Clin Chem* 1986;32:142–5.
- Chiara C, Giovannini I, Siegel JH, Boldrini G, Coleman WP, Castagneto M. Relationship of plasma cholesterol level to doses of branch-chain amino acids in sepsis. *Crit Care Med* 1990;18:32–6.
- Windler E, Ewers-Grabow U, Thiery J, Walli A, Seidel D, Gretern H. The prognostic value of hypocholesterolemia in hospitalized patients. *J Clin Invest* 1994;72:939–43.
- Fraunberger P, Pilz G, Cremer P, Werdan C, Walli AK. Association of serum tumor necrosis factor levels with decrease of cholesterol during septic shock. *Shock* 1998;10:359–63.
- Giovannini I, Boldrini G, Chiara C, Giulianti F, Vellone M, Nuzzo G. Pathophysiologic correlates of hypocholesterolemia in critically ill surgical patients. *Intensive Care Med* 1999;25:748–51.
- Fraunberger P, Nagel D, Walli AK, Seidel D. Serum cholesterol and mortality in patients with multiple organ failure. *Crit Care Med* 2000;28:3574–5.
- Djokovic JL, Hedley-White J. Prediction of outcome of surgery and anesthesia in patients over 80. *JAMA* 1979;242:2301–6.
- Seber GAF. Linear regression analysis. New York: Wiley, 1977:369–82.
- Chijiwa K, Kozaki N, Naito T, Okamoto S, Kuroki H, Yamashita H, et al. Hepatic bile acid synthesis and DNA synthetic rate after partial hepatectomy. *Br J Surg* 1996;83:482–5.
- Akgün S, Ertel NH, Mosenthal A, Oser W. Postsurgical reduction of serum lipoproteins: interleukin-6 and the acute-phase response. *J Lab Clin Med* 1998;131:103–8.
- Cerra FB, Siegel JH, Border JR, Wiles J, McMenamy RR. The hepatic failure of sepsis: cellular vs substrate. *Surgery* 1979;86:409–22.
- Siegel JH, Giovannini I, Coleman B, Cerra FB, Nespoli A. Pathologic synergy in cardiovascular and metabolic compensation with cirrhosis and sepsis. *Arch Surg* 1982;117:225–38.
- Cooper AD. Hepatic lipoprotein and cholesterol metabolism. In: Zakim D, Boyer TD, eds. *Hepatology: a textbook of liver disease*, 2nd ed. Philadelphia: WB Saunders, 1990:96–123.
- Feingold KR, Funk JL, Moser AH, Shigenaga JK, Rapp JH, Grunfeld C. Role for circulating lipoproteins in protection from endotoxin toxicity. *Infect Immun* 1995;63:2041–6.
- Miller NJ, Rice-Evans CA. Spectrophotometric determination of antioxidant activity. *Redox Rep* 1996;2:161–71.
- Muldoon MF, Kritchevsky SB, Evans RW, Kagan VE. Serum total antioxidant activity in relative hypo and hypercholesterolemia. *Free Radic Res* 1996;25:239–45.
- Chiara C, Giovannini I, Siegel JH, Boldrini G, Castagneto M. The relationship between plasma taurine and other amino acid levels in human sepsis. *J Nutr* 2000;130:2222–7.
- Chiara C, Giovannini I, Boldrini G, Castagneto M. The influence of amino acid load and energy expenditure on plasma cholesterol levels in sepsis. *Acta Med Rom* 1989;27:166–70.
- Bakalar B, Zadak Z, Pachi J, Hyspler R, Crhova S. Influence of severe trauma on cholesterol synthesis. *Intensive Care Med* 2000;26(Suppl 3):S357.

**Deletion of the C4-CYP21 Repeat Module Leading to the Formation of a Chimeric CYP21P/CYP21 Gene in a 9.3-kb Fragment as a Cause of Steroid 21-Hydroxylase Deficiency, Hsien-Hsiung Lee,<sup>1\*</sup> Shwu-Fen Chang,<sup>2</sup> Yann-Jinn Lee,<sup>3</sup> Salmo Raskin,<sup>4</sup> Shio-Jean Lin,<sup>5</sup> Mei-Chyn Chao,<sup>6</sup> Fu-Sung Lo,<sup>7</sup> and Ching-Yu Lin,<sup>1</sup>** (<sup>1</sup> King Car Food Industrial Co., Ltd., Yuan-Shan Research Institute, No. 326, Yuan Shan Rd., Sec. 2, Yuan Shan, Ilan 264, Taiwan, Republic of China; <sup>2</sup> Graduate Institute of Cell and Molecular Biology, Taipei Medical University, Taipei 110, Taiwan, Republic of China; <sup>3</sup> Department of Pediatrics, Mackay Memorial Hospital, Taipei 104, and College of Medicine, Taipei Medical University, Taipei 110, Taiwan, Republic of China; <sup>4</sup> Genetika-Centro de Aconselhamento e Laboratorio de Genetica, Curitiba, Parana, Brazil 80410; <sup>5</sup> Department of Pediatrics, College of Medicine, National Cheng Kung University, Tainan 704, Taiwan, Republic of China; <sup>6</sup> Department of Pediatrics, Division of Genetics, Kaohsiung Medical University Hospital, Kaohsiung 807, Taiwan, Republic of China; <sup>7</sup> Division of Endocrinology, Department of Pediatrics, Chang Gung Children's Hospital, Taoyuan 330, Taiwan, Republic of China; \* author for correspondence: fax 886-3-9228030, e-mail hhlee@ms2.kingcar.com.tw)

Gross gene deletions have been reported in 20% of alleles in patients with congenital adrenal hyperplasia (CAH) involving a 21-hydroxylase deficiency (1). This type of deletion occurs in the RCCX module, including the CYP21P, *tenascin A* (TNXA), RP2, C4B, CYP21, and *tenascin B* (TNXB) genes, as evidenced by a 30-kb deletion identified by pulse-field electrophoresis (2). Inactivation of the CYP21 gene may also occur through intergenic recombination with transfer of deleterious mutations from the neighboring CYP21P pseudogene. The frequency of gene deletions or conversions in CAH is controversial (3–5) and is dependent on the population studied. Evidence for gene deletions and/or conversions is traditionally obtained by Southern blot analysis. Multiple probes and separate restriction endonuclease digestions are used. *TaqI* generates 3.7-kb (functional) and 3.2-kb (pseudogene) fragments, and *BglII* produces 11-kb (functional) and 12-kb (pseudogene) fragments. These analyses have been used since 1984 (1, 3, 5–9). However, the method is indirect and time-consuming, and densitometry of fragments can be prone to error.

To identify the interchange region and improve detection of gene deletions and conversions in the RCCX module (10–13), we have developed a novel Southern blot analysis that uses two restriction endonucleases, *AseI* and *NdeI*, and requires only one probe. In addition, we use a PCR product amplified with locus-specific primers covering the TNXB gene to the 5' end of CYP21P or CYP21

to directly analyze the 3.2/3.7-kb *TaqI* fragment and the status of the *CYP21* gene.

For the novel Southern blot analysis, 10  $\mu$ g of genomic DNA was digested with the restriction endonucleases *AseI* and *NdeI*, resolved on a 0.65% agarose gel, blotted on a Hybond-N<sup>+</sup> membrane (Amersham Pharmacia Biotech AB), hybridized with an [ $\alpha$ -<sup>32</sup>P]dCTP-labeled probe, and autoradiographed. The blot was probed with a 2271-bp PCR product amplified with the paired primers Tena36F2/Tena43R. Tena36F2 (5'-AGGCGCTCGCTATGAGGTGAC-3') is located in *TNXB* [nucleotides (nt) 81255–81257; GenBank accession no. AL049547], and Tena43R (5'-CTCCCTTCCTGACCCTCCGCT-3') is located in *TNXB* and *TNXA* (nt 83511–83526; GenBank accession no. AL049547; Fig. 1A).

For PCR amplification, genomic DNA, 0.4 U of *Taq*/*Pow* DNA polymerase (Expand Long Template PCR System; Roche Diagnostics GmbH), primers (7.5 pmol of each), deoxynucleotide triphosphates (200  $\mu$ M each), and 10 $\times$  PCR buffer (commercial supply) were used for PCR amplification in a 30- $\mu$ L reaction. The primers Tena36F2 and CYP749f (Fig. 1A) were used for 6.1-kb PCR product amplification encompassing the *TNXB* gene and the 5' end of the *CYP21* gene. The primer CYP749f (5'-gggtctcctggtggctaaaag-3') is located at the 5' end of the *CYP21P* and *CYP21* genes (nt 87412–87432; GenBank accession no. AL049547). The 6.1-kb PCR product was directly subjected to *TaqI* digestion and analyzed by electrophoresis on 0.65% agarose. For identification of *CYP21* gene status, the PCR product was analyzed by the amplification-created restriction site (ACRS) method (14). The ACRS primer pairing and reaction conditions used for mutation detection, including P30L, IVS-2 -12A/C $\rightarrow$ G, I172N, I236N, V281L, Q318X, and R356W, have been described previously (14).

The strategy for detecting a gene deletion in the RCCX module is shown in Fig. 1A. According to the sequence of the RCCX region among *CYP21P*, *TNXA*, *RP2*, *C4B*, *CYP21*, and *TNXB* obtained from GenBank (accession nos. AF019413 and AL049547) and a restriction map produced by LASERGEN Sequence Analysis Software (DNASTAR), there are two *NdeI* restriction sites. One is located in intron 31 of the *TNXB* gene [nt 77510; GenBank accession no. AL049547; Fig. 1A, (1<sup>st</sup>)] and the other is in exon 8 of the *C4B* gene [nt 101868; GenBank accession no. AL049547; Fig. 1A, (2<sup>nd</sup>)]. There are 11 *AseI* restriction sites in these regions. Nine (Fig. 1A) are in intron 9 of the *C4B* long gene. However, these sites are not present in the *C4A* short gene (15). The other two sites are in exon 16 of the *C4B* gene [nt 99188; GenBank accession no. AL049547; Fig. 1A, (1<sup>st</sup>)] and in the 5' end of the *CYP21P* gene [nt 86855; GenBank accession no. AL049547; Fig. 1A, (11<sup>th</sup>)]. Therefore, the distance between *NdeI* [*TNXB*; Fig. 1A, (1<sup>st</sup>)] and *AseI* [the 5' end of the *CYP21P* gene; Fig. 1A, (11<sup>th</sup>)] is either 38.1 or 43.9 kb, depending on whether *C4B* is present as the long or short form (Fig. 1A). From the map, two fragments of 21.6 and 11.3 kb were obtained by cleavage with *AseI* and *NdeI* in the region as calculated (Fig. 1A). On probe analysis (with Tena36F2/Tena43R),

two fragments of 21.6 and 11.3 kb were obtained in a wild-type individual, as expected (Fig. 1B, lane N). One patient with suspected gene deletions had an additional 9.3-kb fragment as well as the 21.6- and 11.3-kb fragments (Fig. 1B, lane M).

Because the 9.3-kb fragment resulted from gene deletions from the *TNXA*, *RP2*, and *C4B* genes (Fig. 1A), a 6.1-kb PCR product obtained by amplification using the paired primers Tena36F2/CYP749 (Fig. 1A) was derived (Fig. 1D, lane 1) and used to characterize the *CYP21* gene by ACRS analysis. Among 18 CAH families, three types of fused *CYP21* genes were found, designated *CH-1*, *CH-2*, and *CH-3* as shown in Fig. 1C. Both *CH-1* and *CH-2* had been characterized in a previous study (16) (Fig. 1C). On ACRS analysis, *CH-3* had mutations at P30L (Fig. 1C, a), IVS-2 -12A/C $\rightarrow$ G (Fig. 1C, b1), I172N (Fig. 1C, c), I236N (Fig. 1C, d), V281L (Fig. 1C, g), and Q318X (Fig. 1C, j1) as well as nucleotide substitutions at nt -100, -103, -110, and -123 within the promoter region, similar to those of the *CYP21P* gene (data not shown). There was no mutation at R356W in *CH-3* (Fig. 1C, and data not shown). Therefore, these three partial *CYP21P*-like genes were distinct chimeric *CYP21P/CYP21* genes.

To examine the reaction of these three distinct chimeric molecules to *TaqI* digestion, the 6.1-kb PCR product was directly subjected to *TaqI* cleavage analysis. In a wild-type control, 3.7- and 2.4-kb fragments were obtained (Fig. 1D, lane 2). The 2.4-kb fragment is a product of exon 45 (nt 83661; GenBank accession no. AL049547) to intron 36 (nt 81171; GenBank accession no. AL049547) of the *TNXA* and *TNXB* genes. The three chimeric *CYP21P/CYP21* genes, *CH-1* (Fig. 1D, lane 3), *CH-2* (Fig. 1D, lane 4), and *CH-3* (Fig. 1D, lane 5), each contained a 3.2-kb fragment as well as a 3.7-kb fragment.

We have characterized 18 CAH families (17) with a suspected deletion of the *CYP21* gene by one Southern blot using *AseI* and *NdeI* cleavage (data not shown). Each had a 9.3-kb fragment generated by *AseI* and *NdeI* cleavage. The novel Southern analysis with one probe demonstrated that the 9.3-kb fragment is a product of deletion in the RCCX module, including the *XA*, *RP2*, *C4B*, and *CYP21P/CYP21* genes (Fig. 1A). With this method, it is clearly unnecessary to perform a Southern blot twice with both *TaqI* and *BglII* digestions. We therefore suggest that the 9.3-kb fragment is a marker indicating the existence of the chimeric *CYP21P/CYP21* gene. Given the potential for variations and the lack of information about the *C4B* gene (18) in Chinese populations, the size of the RCCX modular deletion may be either 26 or 32 kb (Fig. 1A). The three distinct chimeric *CYP21P/CYP21* genes may result from unequal recombination between the *CYP21P* and *CYP21* genes. We previously suggested (16) that both the *chi*-like sequence GCTGGGG (19) and the tandem-repetitive minisatellite consensus GGGCAGGAXG (20) might be responsible for gene recombination in the formation of *CH-1* and *CH-2*. In the case of *CH-3*, a high congruity of the sequence GGGCAGGACT with GGGCAGGAXG located in intron 7 (nt 1950–1959) probably contributes to the formation of the chimera. We suggest that the base

change from C to T (nt 1994) in Q318X is evidence for a breakpoint of unequal crossover in this case. In addition, we found no *CYP21* gene deletions. We therefore suggest that what has been assumed to be a deletion of the *CYP21* gene may in fact be a chimera.

Southern blot analysis using the *TaqI* restriction endonuclease-generated 3.7- and 3.2-kb fragments for detection of the *CYP21* deletion is time-consuming and involves the use of radioisotopes. Our method is simpler and more convenient in that the 6.1-kb fragment derived

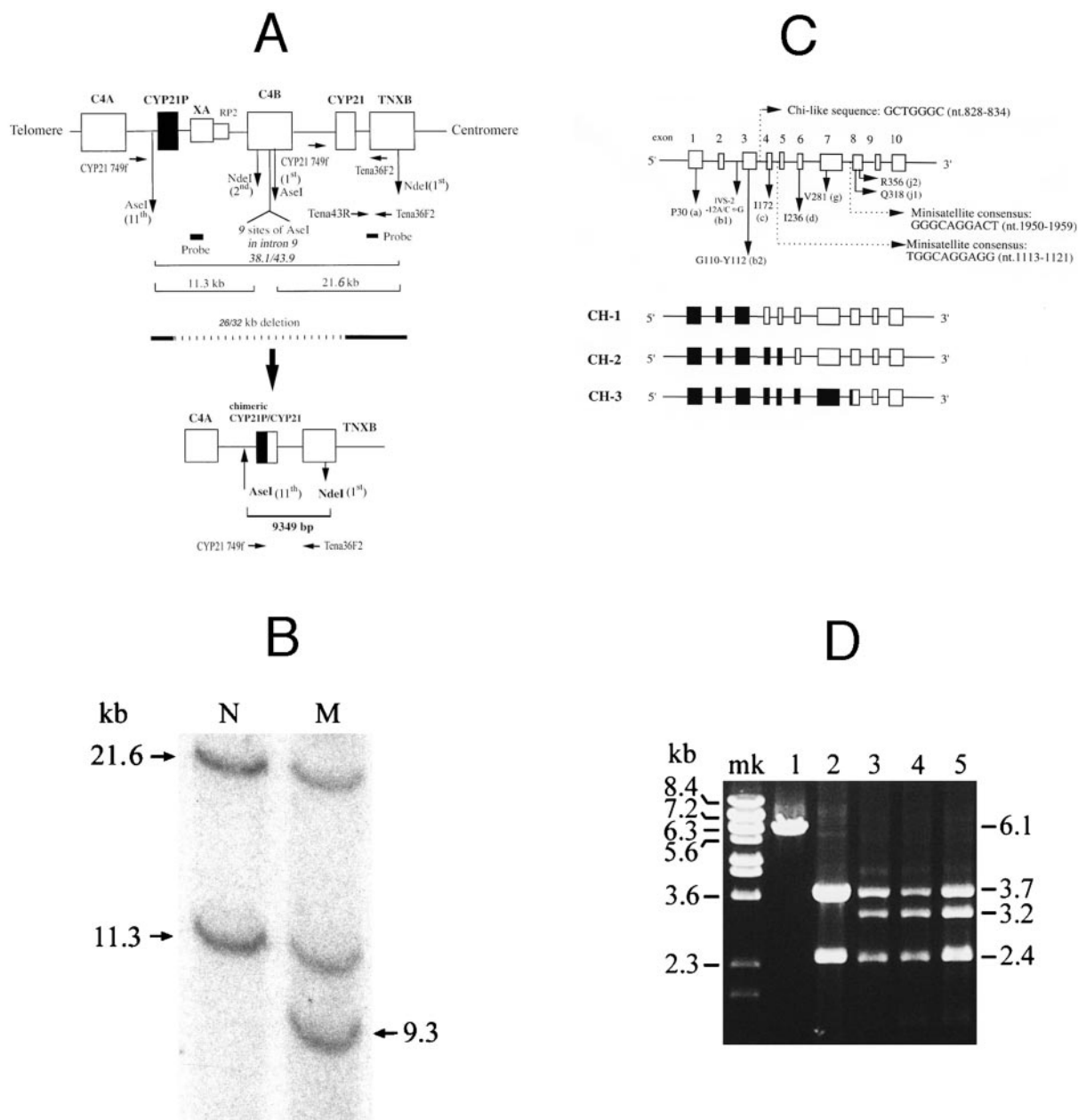


Fig. 1. Strategy for identification of gene deletions in the RCCX module of the human histocompatibility (MHC) class III gene.

(A), the wild-type gene is indicated by □; a nonfunctional gene is indicated by ■. The probe is indicated by the black bar. The deleted region of RCCX is indicated by a solid line, which represents a 26- or 32-kb deletion. The chimeric *CYP21P/CYP21* gene is indicated by ■. Horizontal arrows indicate the direction and location of the primer for PCR amplification, and vertical arrows indicate the location of restriction endonuclease cleavage. (B), Southern blot analysis of *Asel* and *Ndel* digestion products in genomic DNA. Hybridization used the probe consisting of the 2271-bp PCR product derived by the paired primers Tena36F2/Tena43R. A wild-type individual (lane N) had two fragments of 11.3 and 21.6 kb, and 1 of 18 patients suspected of having a gene deletion (lane M) had an additional 9.3-kb fragment as well as the 11.3- and 21.6-kb fragments. (C), detection of an ACRS amplification product for the *CYP21* gene from each locus, designated as (a) for P30L, (b1) for IVS-2 -12A/C → G, (c) for I172N, (d) for I236N, (g) for V281L, (j1) for Q318X, and (j2) for R356W. The structure of the *CYP21* gene is indicated by □, and the *CYP21P* gene is indicated by ■. Solid arrows show the mutation locus in the *CYP21P* gene. Dashed arrows indicate the chi-like sequence and minisatellite consensus as shown in the diagram. CH-1, CH-2, and CH-3 represent three distinct chimeric *CYP21P/CYP21* genes as described in the text. (D), analysis of the *TaqI*-digested 6.1-kb PCR product on a 0.65% agarose gel. Lane 1, 6.1-kb PCR product from a wild-type individual amplified with paired primers Tena36F2/CYP749f; lane 2, *TaqI*-digested 6.1-kb PCR product from a wild-type individual; lanes 3–5, *TaqI*-digested 6.1-kb PCR products from patients with CH-1, CH-2, and CH-3, respectively; lane mk, *Bst*EII-digested lambda DNA marker (New England BioLabs).



by the locus-specific primer is directly subjected to *TaqI* digestion and is analyzed on an agarose gel without radioisotopic hybridization. It also appears to be more accurate because all three distinct chimeric *CYP21P/CYP21* genes had 3.2-kb fragments (Fig. 1C, lanes 3 and 4). Simply assuming that the 3.2-kb fragment from conventional Southern analysis (6) is a deletion of the *CYP21* gene has been shown to be incorrect. The authors of one report have stated that the 3.2-kb fragment analyzed by Southern blotting identified a fused *CYP21* gene, but in this study, Southern blotting was performed with radioisotope hybridization and a different endonuclease (8).

In conclusion, the coexistence of 9.3- and 3.2-kb fragments is consistent with a chimeric *CYP21P/CYP21* gene. The method of analysis we have described is a novel tool for identification of such a molecule. These chimeric genes were found to occur frequently in CAH caused by steroid 21-hydroxylase deficiency in a Taiwanese (ethnic Chinese) population.

We thank Dr. Bun-chu Chung for helpful discussions. This work was supported by the King Car Research Foundation from King Car Food Industrial Cooperation, Taiwan, Republic of China.

## References

- White PC, Vitek A, Dupont B, New MI. Characterization of frequent deletions causing steroid 21-hydroxylase deficiency. *Proc Natl Acad Sci U S A* 1988; 85:4436–40.
- Collier S, Sinnott PJ, Dyer PA, Price DA, Harris R, Strachan T. Pulse field gel electrophoresis identifies a high degree of variability in the number of tandem 21-hydroxylase and complement C4 gene repeats in 21-hydroxylase deficiency haplotypes. *EMBO J* 1989;8:1393–402.
- Matteson KJ, Phillips JA III, Miller WL, Chung BC, Orlando PJ, Frisch H, et al. P450XII (steroid 21-hydroxylase) gene deletions are not found in family studies of congenital adrenal hyperplasia. *Proc Natl Acad Sci U S A* 1987; 84:5858–62.
- Miller WL. Gene conversions, deletions, and polymorphisms in congenital adrenal hyperplasia. *Am J Hum Genet* 1988;42:4–7.
- Morel Y, David M, Forest MG, Betuel H, Hauptman G, Andre J, et al. Gene conversions and rearrangements cause discordance between inheritance of forms of 21-hydroxylase deficiency and HLA types. *J Clin Endocrinol* 1989; 68:592–8.
- White PC, New MI, Dupont B. HLA-linked congenital adrenal hyperplasia results from a defective gene encoding a cytochrome P-450 specific for steroid 21-hydroxylase. *Proc Natl Acad Sci U S A* 1984;81:7505–9.
- Morel Y, Andre J, Uring-Lambert B, Hauptmann G, Betuel H, Tossi M, et al. Rearrangements and point mutations of *P450c21* genes are distinguished by five restriction endonuclease haplotypes identified by a new probing strategy in 57 families with congenital adrenal hyperplasia. *J Clin Invest* 1989;83:527–36.
- Koppens PFJ, Hoogenboezem T, Degenhart HJ. *CYP21* and *CYP21P* variability in steroid 21-hydroxylase deficiency patients and in the general population in the Netherlands. *Eur Hum Genet* 2000;8:827–36.
- L'allemand D, Tardy V, Gruters A, Schnabel D, Krude H, Morel Y. How a patient homozygous for a 30-kb deletion of the *C4-CYP21* genomic region can have a nonclassical form of 21-hydroxylase deficiency. *J Clin Endocrinol Metab* 2000;85:4562–7.
- Gitelman SE, Bristow J, Miller WL. Mechanism and consequences of the duplication of the human *C4/P450c21*/gene X locus. *Mol Cell Biol* 1992; 12:3313–4.
- Bristow J, Tee MK, Gitelman SE, Mellon SH, Miller WL. Tenascin-X: a novel extracellular matrix protein encoded by the human *XB* gene overlapping *P450c21B*. *J Cell Biol* 1993;122:265–78.
- Shen LM, Wu LC, Sanlioglu S, Chen R, Mendoza AR, Dangel A, et al. Structure and genetics of the partially duplicated gene *RP* located immediately upstream of the complement *C4A* and the *C4B* genes in the HLA class III region: molecular cloning, exon-intron structure, composition retroposon and breakpoint of gene duplication. *J Biol Chem* 1994;269:8466–76.
- Yang Z, Mendoza AR, Welch TR, Zipf WB, Yu CY. Modular variations of the human major histocompatibility complex class III genes for serine/threonine kinase *RP*, complement component *C4*, steroid 21-hydroxylase *CYP21*, and tenascin *TNX* (the *RCCX* module). A mechanism for gene deletions and disease associations. *J Biol Chem* 1999;274:12147–56.
- Lee HH, Chao HT, Ng HT, Choo KB. Direct molecular diagnosis of *CYP21* mutations in congenital adrenal hyperplasia. *J Med Genet* 1996;33:371–5.
- Yu CY. The complete exon-intron structure of a human complement component *C4A* gene: DNA sequences, polymorphism, and linkage to the 21-hydroxylase genes. *J Immunol* 1991;146:1057–66.
- Lee HH, Niu DM, Lin RW, Chan P, Lin CY. Structural analysis of the chimeric *CYP21P/CYP21* gene in steroid 21-hydroxylase deficiency. *J Hum Genet* 2002;47:517–22.
- Lee HH, Kuo JM, Chao HT, Lee YJ, Chang JG, Tsai CH, et al. Carrier analysis and prenatal diagnosis of congenital adrenal hyperplasia due to 21-hydroxylase deficiency in Chinese. *J Clin Endocrinol Metab* 2000;85:597–600.
- Yang Z, Shen L, Dangel AW, Wu LC, Yu CY. Four ubiquitously expressed genes, *RD* (D6S45)-*SK12W*-(*SKIV2L*)-*DOM3Z*-*RP1*(*D6S60E*), are present between complement component genes factor B and C4 in the class III region of the HLA. *Genomics* 1998;53:338–47.
- Smith GR, Kunes SM, Schultz DW, Taylor A, Triman KL. Structure of *chi* hotspots of generalized recombination. *Cell* 1981;24:429–36.
- Jeffreys AJ, Wilson V, Thein SL. Hypervariable 'minisatellite' regions in human DNA. *Nature* 1985;314:67–73.

**Rapid HPLC-Electrospray Tandem Mass Spectrometric Assay for Urinary Testosterone and Dihydrotestosterone Glucuronides from Patients with Benign Prostate Hyperplasia, Man Ho Choi,<sup>1\*</sup> Jung Nyun Kim,<sup>2</sup> and Bong Chul Chung<sup>1†</sup>** (<sup>1</sup>Bioanalysis & Biotransformation Research Center, KIST, Seoul 130-650, Korea; <sup>2</sup>Division of Food Investigation, Korea Advanced Food Research Institute, Seoul 137-060, Korea; \* current address: Division of Bio-engineering & Environmental Health, Massachusetts Institute of Technology, Cambridge, MA 02139; † address correspondence to this author at: Bioanalysis & Biotransformation Research Center, Korea Institute of Science and Technology, PO Box 131, Cheongryang, Seoul 130-650, Korea; fax 82-2-958-5059, e-mail bcc0319@kist.re.kr)

The development of benign prostatic hyperplasia (BPH) is dependent on androgens, primarily dihydrotestosterone (DHT) (1). To estimate the activity of 5 $\alpha$ -reductase, which catalyzes the conversion of testosterone to DHT, testosterone and DHT have been quantified in biological samples (2–4). Because of their lipophilic properties, they are usually found in the conjugated form, i.e., linked to a hydrophilic sulfuric moiety or  $\beta$ -glucuronic acid, which are excreted mainly (>95%) in human urine. Despite reports of a close association between BPH and testosterone and DHT (1–4), to our knowledge, there is no published simultaneous quantitative data for these metabolites as their glucuronides in the urine of patients with BPH.

The major problem associated with quantification of total steroids is incomplete hydrolysis, attributable mainly to the matrix effects of urine on the efficiency of enzymatic hydrolysis, which reduces the reproducibility of the assay (5,6). Given that it is often necessary to analyze many samples in a short time with good sensitivity and reproducibility, system throughput is a critical issue for many clinical mass spectrometry (MS) groups. In